THE VARIANCE METHOD OF PREDICTING THE FATIGUE FRACTURE PLANE UNDER MULTIAXIAL RANDOM LOADINGS

W.Będkowski, C.Lachowicz, E.Macha
Technical University of Opole,ul.ZSP 5,45-851 Opole, Poland

Third International Conference on Biaxial/Multiaxial Fatigue
3-6 April 1989, Stuttgart, FRG

Abstract. It is assumed that the plane in which the maximum variance of the equivalent stress appears is critical for a material and the fatigue fracture should be expected in this plane. The equivalent stress is calculated according to the fatigue criterion of maximum shear and normal stresses in the fracture plane. It was demonstrated that for each stationary random stress state there is one or more critical planes where the fatigue fracture plane can be expected.

1. INTRODUCTION

Positions of fatigue fracture planes (macro) under multiaxial sinusoidal loadings are dependent-among others-on:

- a state of material (elastic-brittle or elastic-plastic materials) [1,5,11],
- ratio of amplitudes of stress state components [5,11],
- a value of amplitudes (low-cycle fatigue ,high-cycle fatigue) [13],
- phase displacements [2,10,11,15].

For elastic-brittle materials the fatigue fracture plane is often perpendicular to the direction of the normal stress with the maximum amplitude. For materials in elastic-plastic state the fracture plane is often one of two planes where shear stresses have the maximum amplitude. There are also intermediate positions of fatigue fracture planes.

Under multiaxial random loadings predominant damage mechanisms and factors influencing the fatigue fracture plane position can be expressed with averaging, i.e. evaluation of some statistical parameters. For these conditions three methods of determination of the expected fatigue fracture plane position can be proposed [9]:

- method of weight functions [1],

- method of variance [2,3,4],
- method of damage cumulation [9].

These methods:

- concern random states of stress components of which are stationary and ergodic Gaussian stochastic processes,
- take random changes of directions of principal stress axes into account,
- use relation $\sigma_1(t)\geq\sigma_2(t)\geq\sigma_3(t)$ at any time t for defining random values and directions of principal stresses,
- allow to determine the expected fatigue fracture plane position with the unit vector normal to the discussed plane $\bar{\eta}$ with components dependent on the mean direction cosines $\hat{l}_n$, $\hat{m}_n$, $\hat{n}_n$, (n= = 1,2,3) of axes of principal stresses.

Till now the method of variance has been connected with the criteria of:

- maximum normal stress in the fracture plane [4],
- maximum strain in direction perpendicular to the fracture plane [3],
- maximum shear stress in the fracture plane [2].

In this paper application of the variance method is presented in connection with a more general criterion of maximum shear and normal stresses in the fracture plane [7].

2. FATIGUE CRITERION OF MAXIMUM SHEAR AND NORMAL STRESSES IN A FRACTURE PLANE

It is assumed that:

1. Fatigue fracture is caused by the normal stresses $\sigma_\eta(t)$ and shear stresses $\tau_{\eta s}(t)$ acting in the $\bar{s}$ direction on a fracture plane with a normal $\bar{\eta}$.
2. The direction $\bar{s}$ on the fracture plane coincides with the mean direction of the maximum shear stress $\tau_{\eta max}(t)$.
3. In a limit state conforming to fatigue strength the maximum value of combination of stresses $\tau_{\eta s}(t)$ and $\sigma_\eta(t)$ under multiaxial random loadings satisfies the following equation:

$$\max_t \{\tau_{\eta s}(t) + K\sigma_\eta(t)\} = F \tag{1}$$

where K,F - material constants determined during cyclic fatigue tests.

If we assume that the expected fracture plane is determined by the mean position of one of two planes of the maximum shear stress $\tau_\eta(t)$ and the direction $\bar{s}$ coincident with the mean position of stress $\tau_1(t)$ we obtain the following form of equivalent stress:

$$\sigma_{red}(t) = \frac{1}{1+K} [(\hat{l}_1^2 - \hat{l}_3^2 + K(\hat{l}_1 + \hat{l}_3)^2)\sigma_{xx}(t) + (\hat{m}_1^2 - \hat{m}_3^2 + K(\hat{m}_1 + \hat{m}_3)^2)\sigma_{yy}(t) + (\hat{n}_1^2 - \hat{n}_3^2 + K(\hat{n}_1 + \hat{n}_3)^2)\sigma_{zz}(t) + 2(\hat{l}_1\hat{m}_1 - \hat{l}_3\hat{m}_3 + K(\hat{l}_1 + \hat{l}_3)(\hat{m}_1 + \hat{m}_3))\sigma_{xy}(t) + 2(\hat{l}_1\hat{n}_1 - \hat{l}_3\hat{n}_3 + K(\hat{l}_1 + \hat{l}_3)(\hat{n}_1 + \hat{n}_3))\sigma_{xz}(t) + 2(\hat{m}_1\hat{n}_1 - \hat{m}_3\hat{n}_3 + K(\hat{m}_1 + \hat{m}_3)(\hat{n}_1 + \hat{n}_3))\sigma_{yz}(t)] \quad (2)$$

where $\sigma_{ij}(t), (i,j=x,y,z)$ - stress state components.

$$\bar{\eta} = \frac{\hat{l}_1 + \hat{l}_3}{\sqrt{2}}\bar{i} + \frac{\hat{m}_1 + \hat{m}_3}{\sqrt{2}}\hat{j} + \frac{\hat{n}_1 + \hat{n}_3}{\sqrt{2}}\bar{k}$$

$$\bar{s} = \frac{\hat{l}_1 - \hat{l}_3}{\sqrt{2}}\bar{i} + \frac{\hat{m}_1 - \hat{m}_3}{\sqrt{2}}\bar{j} + \frac{\hat{n}_1 - \hat{n}_3}{\sqrt{2}}\bar{k}$$

The mean direction cosines should satisfy the following conditions of orthogonality:

$$\hat{l}_n^2 + \hat{m}_n^2 + \hat{n}_n^2 = 1, \quad (n=1,2,3)$$

$$\hat{l}_1\hat{l}_2 + \hat{m}_1\hat{m}_2 + \hat{n}_1\hat{n}_2 = 0, \qquad \hat{l}_1\hat{l}_3 + \hat{m}_1\hat{m}_3 + \hat{n}_1\hat{n}_3 = 0$$

$$\hat{l}_2\hat{l}_3 + \hat{m}_2\hat{m}_3 + \hat{n}_2\hat{n}_3 = 0 \quad (3)$$

In case of multiaxial cyclic loadings Findley et al [6], Stulen and Cummings [14] assumed that the normal of the critical shear plane (fracture plane) $\bar{\eta}$ formed an angle θ with the direction of the normal stress having the maximum amplitude and a coefficient K can be calculated from

$$\frac{\sigma_{af}}{\tau_{af}} = \frac{2}{1 + \frac{1}{\sqrt{1+K^2}}} \quad \text{or } \mathrm{tg}\, 2\theta = \frac{1}{K}$$

where σ_{af} - fatigue limit under tension-compression, τ_{af} - fatigue limit under torsion. Thus

$$K = \sqrt{\left(\frac{\sigma_{af}}{2\,\tau_{af} - \sigma_{af}}\right)^2 - 1} \qquad \text{or} \quad K = \frac{1}{tg\ 2\theta} \tag{4}$$

From formula (2) it appears that the equivalent stress $\sigma_{red}(t)$ is linearly dependent on the stress state components $\sigma_{ij}(t)$ so it can be expressed as

$$\sigma_{red}(t) = \sum_{k=1}^{6} a_k x_k\ (t) \tag{5}$$

where

$x_1(t) = \sigma_{xx}(t)$, $\quad x_4(t) = \sigma_{xy}(t)$
$x_2(t) = \sigma_{yy}(t)$, $\quad x_5(t) = \sigma_{xz}(t)$
$x_3(t) = \sigma_{zz}(t)$, $\quad x_6(t) = \sigma_{yz}(t)$

and a_k is constant coefficient.
The expected value of the equivalent stress $\hat{\sigma}_{red}$ can be calculated from the following formula

$$\hat{\sigma}_{red} = \sum_{k=1}^{6} a_k\ \hat{x}_k \tag{6}$$

where $\hat{x}_k$ - the expected value of stress state components $x_k(t)$.

In this paper we assume that stress state components have their expected values equal to zero,then,according to (6),the expected value of the equivalent stress is equal to zero as well, i.e. $\hat{\sigma}_{red}=0$. The variance of the equivalent stress $\mu_{\sigma red}$ is an important parameter determining fatigue life. It can be calculated from

$$\mu_{\sigma red} = \sum_{s=1}^{6} \sum_{t=1}^{6} a_s\ a_t\ \mu_{xst} \tag{7}$$

where a_s, a_t are the same coefficients as a_k in (6), they are suitably chosen for elements μ_{xst} of the covariance matrix of random variables x_k. After transformations the equivalent stress variance is equal to

$$\mu_{\sigma red} = \frac{1}{(1+K)^2} \{[\hat{l}_1{}^2-\hat{l}_3{}^2+ K(\hat{l}_1 +\hat{l}_3)^2]^2\ \mu_{x11}+ [\hat{m}_1{}^2-\hat{m}_3{}^2+ K\ (\hat{m}_1 + \hat{m}_3)^2]^2\ \mu_{x22}+ [\hat{n}_1{}^2-\hat{n}_3{}^2+ K\ (\hat{n}_1+\hat{n}_3)^2]^2\ \mu_{x33}+ 4\ [\hat{l}_1\hat{m}_1- \hat{l}_3\hat{m}_3+ K\ (\hat{l}_1+ \hat{l}_3)(\hat{m}_1+\hat{m}_3)]^2\ \mu_{x44}+ 4\ [\hat{l}_1\hat{n}_1-\hat{l}_3\hat{n}_3+ K\ (\hat{l}_1+\hat{l}_3)(\hat{n}_1+\hat{n}_3)]^2\ \mu_{x55}+ 4\ [\hat{m}_1\hat{n}_1- -\hat{m}_3\hat{n}_3+ K\ (\hat{m}_1+\hat{m}_3)(\hat{n}_1+\hat{n}_3)]^2\ \mu_{x66}+ 2\ [\hat{l}_1{}^2-\hat{l}_3{}^2)+K\ (\hat{l}_1+\hat{l}_3)^2][\hat{m}_1{}^2- \hat{m}_3{}^2 + K(\hat{m}_1+\hat{m}_3)^2]\mu_{x12}+ 2\ [\hat{l}_1{}^2-\hat{l}_3{}^2)+ K(\hat{l}_1+\hat{l}_3)^2][\hat{n}_1{}^2-\hat{n}_3{}^2+ K(\hat{n}_1+\hat{n}_3)^2]\ \mu_{x13} +$$

$$4[\hat{l}_1{}^2-\hat{l}_3{}^2+ K(\hat{l}_1+\hat{l}_3)^2][\hat{l}_1\hat{m}_1-\hat{l}_3\hat{m}_3+ K(\hat{l}_1+\hat{l}_3)(\hat{m}_1+\hat{m}_3)]\mu_{x14}+4 [\hat{l}_1{}^2-\hat{l}_3{}^2 + K (\hat{l}_1+\hat{l}_3)^2][\hat{l}_1\hat{n}_1-\hat{l}_3\hat{n}_3+ K(\hat{l}_1+\hat{l}_3)(\hat{n}_1+\hat{n}_3)]\mu_{x15}+4 [\hat{l}_1{}^2-\hat{l}_3{}^2+ K(\hat{l}_1+\hat{l}_3)^2] [\hat{m}_1\hat{n}_1-\hat{m}_3\hat{n}_3+ K (\hat{m}_1+\hat{m}_3)(\hat{n}_1+\hat{n}_3)]\mu_{x16}+ 2 [\hat{m}_1{}^2-\hat{m}_3^2)+ K (\hat{m}_1+\hat{m}_3)^2] [\hat{n}_1{}^2-\hat{n}_3{}^2+K (\hat{n}_1+\hat{n}_3)^2]\mu_{x23}+ 4 [\hat{m}_1{}^2-\hat{m}_3{}^2+ K (\hat{m}_1+\hat{m}_3)^2][\hat{l}_1\hat{m}_1-\hat{l}_3\hat{m}_3+ K (\hat{l}_1+\hat{l}_3)(\hat{m}_1+\hat{m}_3)]\mu_{x24}+ 4 [\hat{m}_1{}^2-\hat{m}_3{}^2+ K(\hat{m}_1+\hat{m}_3)^2][\hat{l}_1\hat{n}_1-\hat{l}_3\hat{n}_3+ K (\hat{l}_1+\hat{l}_3)(\hat{n}_1+\hat{n}_3)]\mu_{x25}+ 4 [\hat{m}_1{}^2-\hat{m}_3{}^2+ K (\hat{m}_1+\hat{m}_3)^2][\hat{m}_1\hat{n}_1-\hat{m}_3\hat{n}_3+ K (\hat{m}_1+\hat{m}_3) (\hat{n}_1+ \hat{n}_3)]\mu_{x26}$$

$$4 [\hat{n}_1{}^2- \hat{n}_3{}^2 + K (\hat{n}_1+ \hat{n}_3)^2] [\hat{l}_1\hat{m}_1- \hat{l}_3\hat{m}_3 + K (\hat{l}_1+ \hat{l}_3) (\hat{m}_1+\hat{m}_3)]\mu_{x34}+ 4 [\hat{n}_1{}^2- \hat{n}_3{}^2+ K (\hat{n}_1+ \hat{n}_3)^2] [\hat{l}_1\hat{n}_1- \hat{l}_3\hat{n}_3 + K (\hat{l}_1+ \hat{l}_3) (\hat{n}_1+ \hat{n}_3)]\mu_{x35}+ 4 [\hat{n}_1{}^2- \hat{n}_3{}^2+ K (\hat{n}_1+ \hat{n}_3)^2] [\hat{m}_1\hat{n}_1- \hat{m}_3\hat{n}_3 + K (\hat{m}_1+ \hat{m}_3) (\hat{n}_1+ \hat{n}_3)]\mu_{x36}+ 8 [\hat{l}_1\hat{m}_1-\hat{l}_3\hat{m}_3+ K (\hat{l}_1+\hat{l}_3)(\hat{m}_1+\hat{m}_3)][\hat{l}_1\hat{n}_1-\hat{l}_3\hat{n}_3+ K (\hat{l}_1+\hat{l}_3)(\hat{n}_1+\hat{n}_3)]\mu_{x45}+ 8 [\hat{l}_1\hat{m}_1-\hat{l}_3\hat{m}_3+ K (\hat{l}_1+\hat{l}_3)(\hat{m}_1+\hat{m}_3)][\hat{m}_1\hat{n}_1-\hat{m}_3\hat{n}_3+ K (\hat{m}_1+\hat{m}_3)(\hat{n}_1+\hat{n}_3)]\mu_{x46}+ 8 [\hat{l}_1\hat{n}_1-\hat{l}_3\hat{n}_3+ K (\hat{l}_1+\hat{l}_3)(\hat{n}_1+\hat{n}_3)][\hat{m}_1\hat{n}_1-\hat{m}_3\hat{n}_3+ K(\hat{m}_1+\hat{m}_3)(\hat{n}_1+\hat{n}_3)]\mu_{x56}\} \quad (8)$$

3. METHOD OF VARIANCE

The method of variance is based on the assumption that the plane in which variance of the equivalent stress reaches its maximum is critical for a material and fatigue fracture should be expected in this plane.

For stationary stochastic loadings, i.e. for determined values of elements of the covariance matrix μ_{xst}, the variance $\mu_{\sigma red}$ depends on 6 directional cosines $\hat{l}_n$, $\hat{m}_n$, $\hat{n}_n$, (n=1,2,3) which must fulfill orthogonality conditions (3). In such a case searching the maximum variance (8) is quite difficult. The conditional maximum of a non-linear function of several variables with non-linear limitations (3) should be found. Unfortunately, the problem cannot be simply analitically solved in a general case. In order to eliminate these difficulties directional cosines $\hat{l}_n, \hat{m}_n, \hat{n}_n$ are replaced by trigonometric functions of three Euler angles $\hat{\vartheta}, \hat{\Phi}, \hat{\varphi}$ in the following way

$$\hat{l}_1 = \cos\hat{\psi}\cos\hat{\phi} - \cos\hat{\vartheta}\sin\hat{\psi}\sin\hat{\phi},$$
$$\hat{m}_1 = \sin\hat{\psi}\cos\hat{\phi} + \cos\hat{\vartheta}\cos\hat{\psi}\sin\hat{\phi},$$
$$\hat{n}_1 = \sin\hat{\vartheta}\sin\hat{\phi}$$
$$\hat{l}_2 = -\cos\hat{\psi}\sin\hat{\phi} - \cos\hat{\vartheta}\sin\hat{\psi}\cos\hat{\phi}, \qquad (9)$$
$$\hat{m}_2 = -\sin\hat{\psi}\sin\hat{\phi} + \cos\hat{\vartheta}\cos\hat{\psi}\cos\hat{\phi},$$
$$\hat{n}_2 = \sin\hat{\vartheta}\cos\hat{\phi},$$
$$\hat{l}_3 = \sin\hat{\vartheta}\sin\hat{\psi}, \quad \hat{m}_3 = -\sin\hat{\vartheta}\cos\hat{\psi}, \quad n_3 = \cos\hat{\vartheta}$$

where $0 \le \hat{\vartheta} < \pi$, $0 \le \hat{\psi} < 2\pi$, $0 \le \hat{\phi} < 2\pi$

Thus, a number of six dependent parameters was reduced to three independent ones determining the variance of equivalent stress

$$\mu_{\sigma red} = f(\hat{\vartheta}, \hat{\psi}, \hat{\phi}, K, \mu_{xst}) \qquad (10)$$

The orthogonality conditions (3) were also eliminated.

Searching the maximum of nonlinear function (10) in an analytical way is still, in many cases, not effective.

The digital simulation method was used in order to investigate courses of variability of function (10) depending on the mean values of Euler angles $\hat{\vartheta}$, $\hat{\psi}$, $\hat{\phi}$, (μ_{xst} and K are constants).

The maximum variance (10) was also numerically calculated with a suitable method of nonlinear optimization function of many variables (complex method). The schematic algorithm of the variance method for determination of the expected fatigue fracture plane position is presented in Fig. 1.

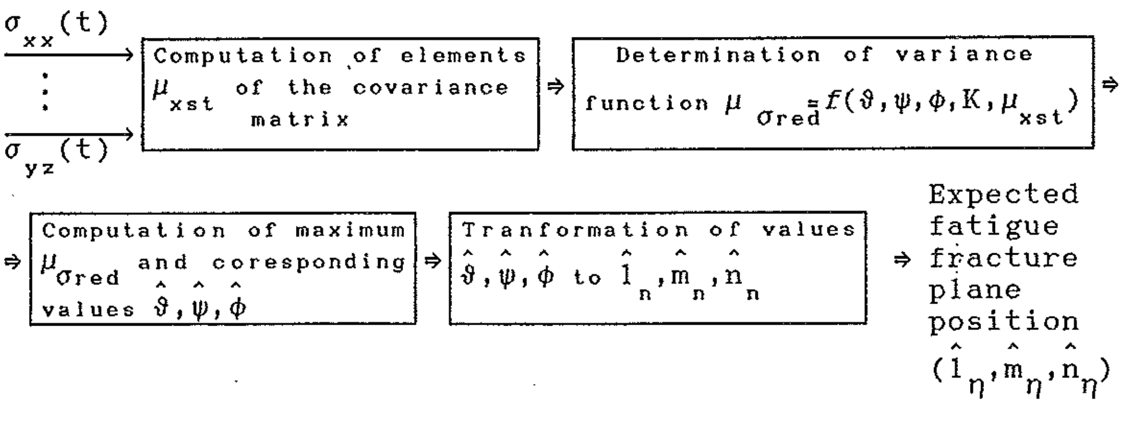

Fig.1 Algorithm of the variance method for determination of the expected fatigue fracture plane position

4. THE EXPECTED LOCATIONS OF FATIGUE FRACTURE PLANES

On the basis of the presented method the expected fatigue fracture plane position is determined for four simulated random states of stress. The uncorrelated components of the random stress state are generated as sequences of random numbers with normal probability distribution $N(0, \mu_x)$ and wide-band frequency spectrum [8]. Calculations are made for two different materials:

-mild steel (0.1%C), $\sigma_{af}=203$ MPa, $\tau_{af}=180$ MPa, K=0.8197

-Swedish hard steel (0.51%C), $\sigma_{af}=313.9$ MPa, $\tau_{af}=196.2$ MPa, K=3.8717.

4.1 Uniaxial tension-compression

With the condition that $\sigma_{xx}(t) \neq 0$ and vanishingg the remaining stresses $\sigma_{ij}(t)=0$ for i,j=x,y,z,it can be shown that

$$\mu_{\sigma red} = \frac{1}{(1+K)^2} \left[\hat{l}_1^{\,2} - \hat{l}_3^{\,2} + K(\hat{l}_1 + \hat{l}_3)^2\right]^2 \mu_{x11} \qquad (11)$$

The generated course $\sigma_{xx}(t)$ with variance $\mu_{x11}=3888$ MPa^2 gives the maximum of variance $\mu_{\sigma red}=5241$ MPa^2 for mild steel and $\mu_{\sigma red}=$ $=10148$ MPa^2 for hard steel when the cosines have the following values:

I. Mild steel

$\hat{l}_1$	$\hat{m}_1$	$\hat{n}_1$	$\hat{l}_3$	$\hat{m}_3$	$\hat{n}_3$
± 0.9417	m_{1I}	$\pm\sqrt{0.1132-m_{1I}^{\,2}}$	± 0.3366	m_{3I}	$\pm\sqrt{0.8867-m_{3I}^{\,2}}$
but	$m_{1I}^{\,2} \le 0.1132$			$m_{3I}^{\,2} \le 0.8867$	
then $\hat{l}_\eta$	$\hat{m}_\eta$	$\hat{n}_\eta$	$\hat{l}_s$	$\hat{m}_s$	$\hat{n}_s$
± 0.9039	$m_{\eta I}$	$\pm\sqrt{0.1830-m_{\eta I}^{\,2}}$	± 0.4279	m_{sI}	$\pm\sqrt{0.8169-m_{sI}^{\,2}}$
	$m_{\eta I}^{\,2} \le 0.1830$			$m_{sI}^{\,2} \le 0.8169$	

II. Hardened steel

$\hat{l}_1$	$\hat{m}_1$	$\hat{n}_1$	$\hat{l}_3$	$\hat{m}_3$	$\hat{n}_3$
± 0.7906	m_{1II}	$\pm\sqrt{0.3750-m_{1II}^{\,2}}$	± 0.6123	m_{3II}	$\pm\sqrt{0.6251-m_{3II}^{\,2}}$
but	$m_{1II}^{\,2} \le 0.375$			$m_{3II}^{\,2} \le 0.6251$, so	
$\hat{l}_\eta$	$\hat{m}_\eta$	$\hat{n}_\eta$	$\hat{l}_s$	$\hat{m}_s$	$\hat{n}_s$
± 0.9920	$m_{\eta II}$	$\pm\sqrt{0.0159-m_{\eta II}^{\,2}}$	± 0.1261	m_{sII}	$\pm\sqrt{0.9841-m_{sII}^{\,2}}$
but	$m_{\eta II}^{\,2} \le 0.0159$			$m_{sII}^{\,2} \le 0.9841$	

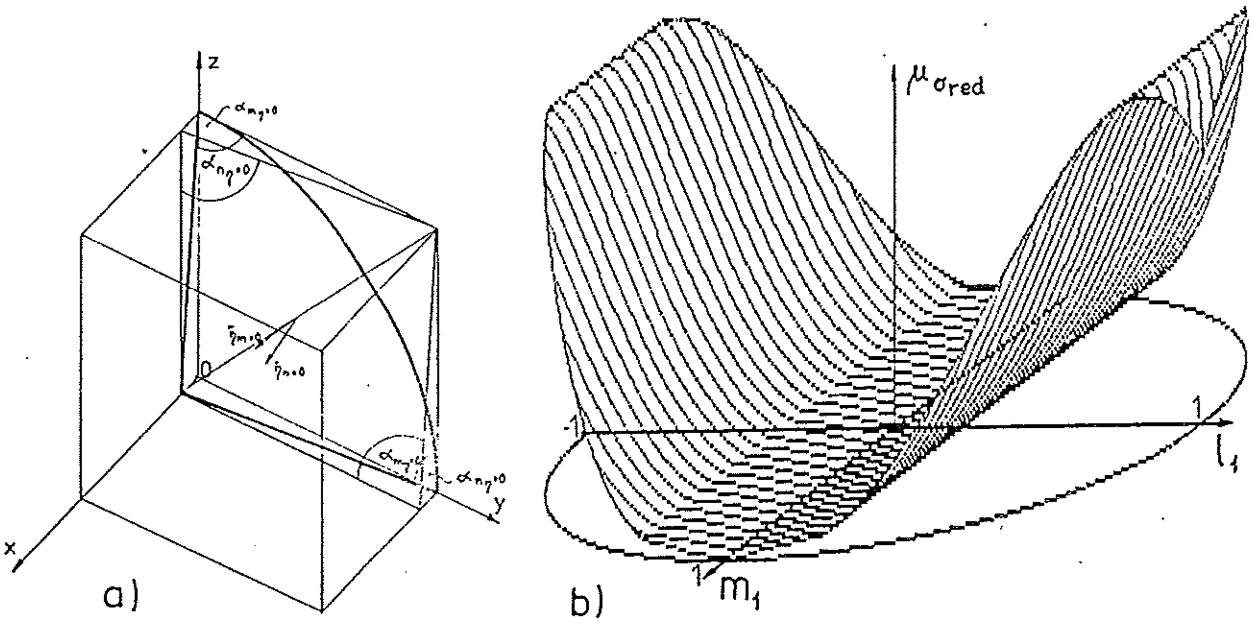

Fig. 2I The expected fatigue fracture plane positions and a graph of variance function (according to(11))for mild steel

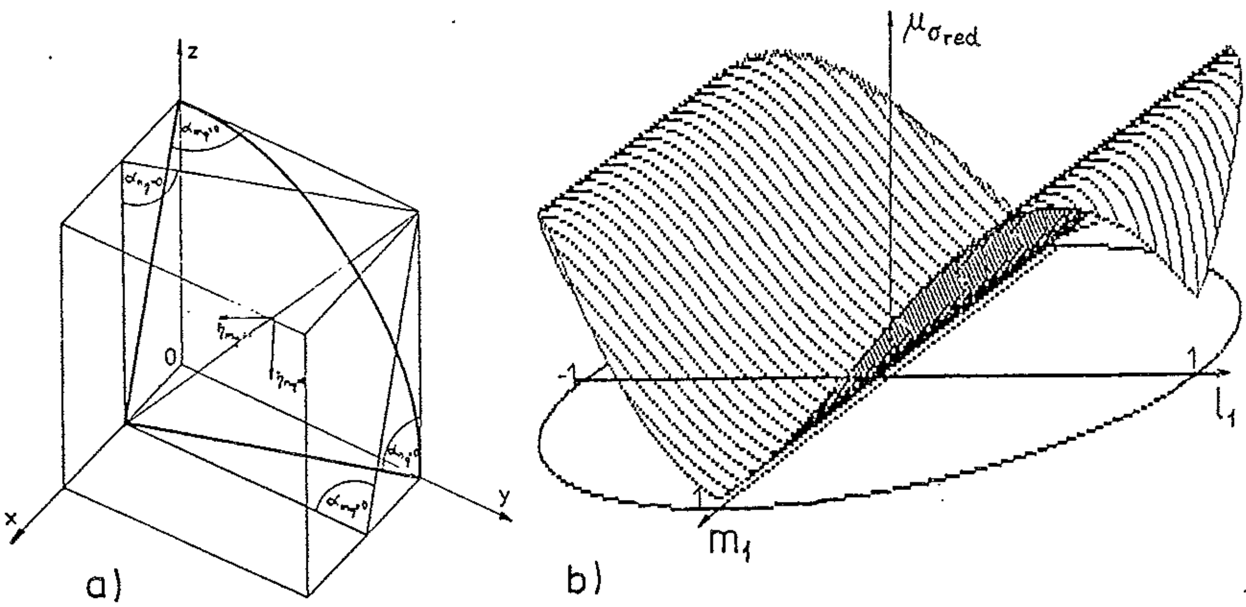

Fig. 2II The expected fatigue fracture plane positions and a graph of variance function (according to(11))for hard steel

The expected fatigue fracture plane positions are presented in Figs. 2Ia and 2IIa. Figs.2Ib and 2IIb show a graph of function $\mu_{\sigma red}$ in the system of axes $\hat{l}_1, \hat{m}_1$ (the remaining cosines are selected taking into account orthogonality conditions and so as to reach the maximum value of $\mu_{\sigma red}$).

The infinite number of planes inclined to the axis x at the following angles

I. $\alpha_{\eta I} = 64^o\ 41'$ for mild steel

II. $\alpha_{\eta II} = 82^o\ 45'$ for hard steel

have been obtained.

There is a distinct influence of a kind of material (constant K) on location of the expected fracture plane. For hard steel the direction $\bar{\eta}$ forms a smaller angle with the direction of stress $\sigma_{xx}(t)$ than for mild steel

4.2 Biaxial tension-compression with shear

The conditions for biaxial tension-compression with shear are: $\sigma_{xx}(t) \neq 0$, $\sigma_{yy}(t) \neq 0$, $\sigma_{xy}(t) \neq 0$ and $\sigma_{ij}(t) = 0$ for i,j = x, y,z. This leads to

$$\mu_{\sigma red} = \frac{1}{(1+K)^2} \{ [\hat{l}_1^2 - \hat{l}_3^2 + K (\hat{l}_1 + \hat{l}_3)^2]^2 \mu_{x11} + [\hat{m}_1^2 - \hat{m}_3^2 +$$

$$+K (\hat{m}_1 + \hat{m}_3)^2]^2 \mu_{x22} + 4 [\hat{l}_1\hat{m}_1 - \hat{l}_3\hat{m}_3 + K (\hat{l}_1 + \hat{l}_3) (\hat{m}_1 + \hat{m}_3)]^2 \mu_{x44} +$$

$$+ 2 [\hat{l}_1^2 - \hat{l}_3^2 + K (\hat{l}_1 + \hat{l}_3)^2] [\hat{m}_1^2 - \hat{m}_3^2 + K (\hat{m}_1 + \hat{m}_3)^2] \mu_{x12} +$$

$$+ 2 [\hat{l}_1^2 - \hat{l}_3^2 + K (\hat{l}_1 + \hat{l}_3)^2] [\hat{l}_1\hat{m}_1 - \hat{l}_3\hat{m}_3 + K (\hat{l}_1 + \hat{l}_3) (\hat{m}_1 + \hat{m}_3)]$$

$$\mu_{x44} + 4 [\hat{m}_1^2 - \hat{m}_3^2 + K (\hat{m}_1 + \hat{m}_3)^2] [\hat{l}_1\hat{m}_1 - \hat{l}_3\hat{m}_3 + K (\hat{l}_1 + \hat{l}_3)$$

$$(\hat{m}_1 + \hat{m}_3)] \mu_{x24}\} \qquad (12)$$

The calculated covarriance matrix for the generated components of stress state is equal to

$$\underset{\approx}{\mu}_x = \begin{vmatrix} \mu_{x11}, \mu_{x12}, \mu_{x14} \\ \mu_{x21}, \mu_{x22}, \mu_{x24} \\ \mu_{x41}, \mu_{x42}, \mu_{x44} \end{vmatrix} = \begin{vmatrix} 3872 & 7 & -2 \\ 7 & 3899 & -9 \\ -2 & -9 & 3840 \end{vmatrix}$$

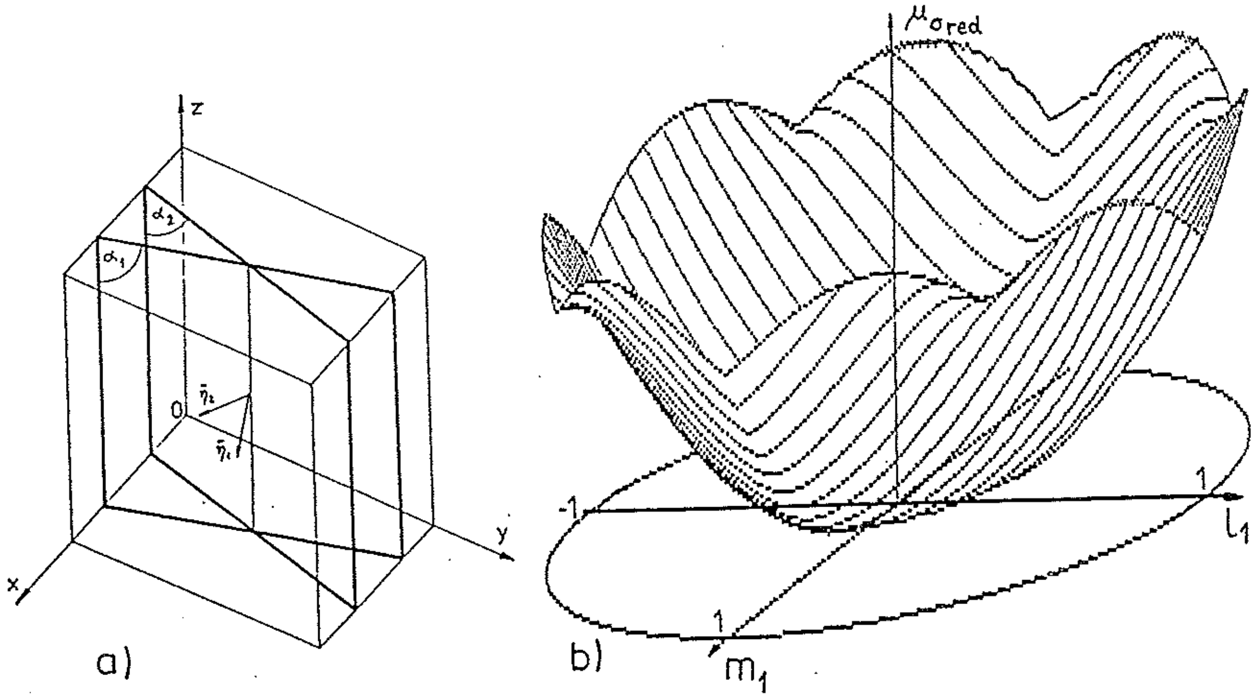

Fig. 3I The expected fatigue fracture plane positions and a graph of variance function (according to 12) for mild steel

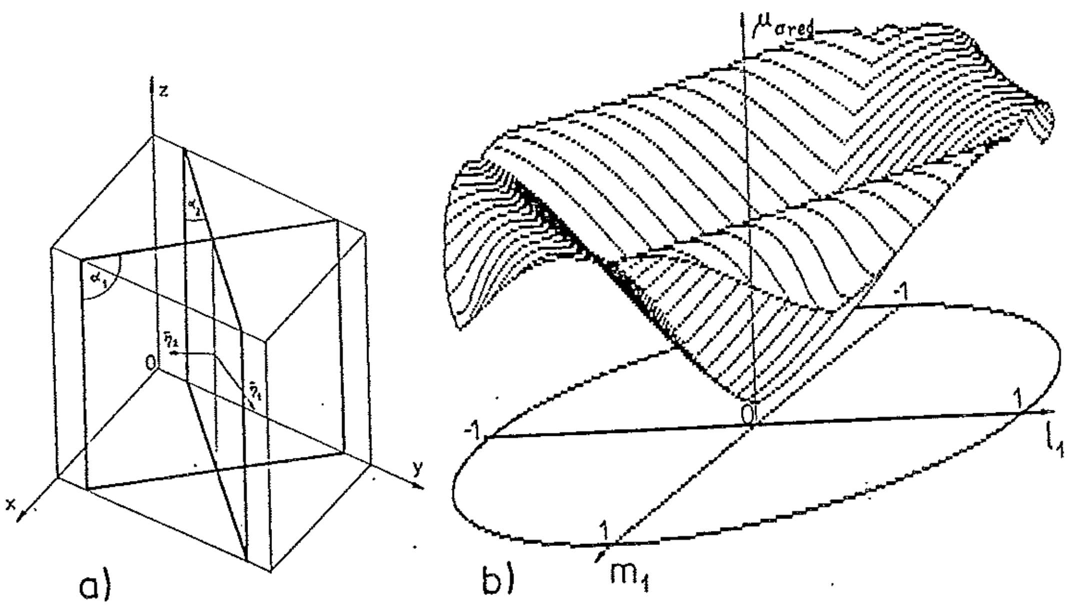

Fig. 3II The expected fatigue fracture plane positions and a graph of variance function (according to 12) for hard steel

From optimization procedure maximum of the function (12) $\mu_{\sigma red}$ = =9347 MPa^2 for mild steel and $\mu_{\sigma red}$=15298 MPa^2 for hard steel where obtained; values of the direction cosines were the following .

I.Mild steel

$\hat{l}_1$	$\hat{m}_1$	$\hat{n}_1$	$\hat{l}_3$	$\hat{m}_3$	$\hat{n}_3$
±0.4269	±0.9043	0.0	±0.9043	∓0.4268	0.0
±0.4269	∓0.9043	0.0	±0.9043	±0.4268	0.0

then

$\hat{l}_\eta$	$\hat{m}_\eta$	$\hat{n}_\eta$	$\hat{l}_s$	$\hat{m}_s$	$\hat{n}_s$
±0.9413	±0.3376	0.0	∓0.3376	±0.9413	0.0
±0.9413	∓0.3376	0.0	∓0.3376	∓0.9413	0.0

II. Hardened steel

$\hat{l}_1$	$\hat{m}_1$	$\hat{n}_1$	$\hat{l}_3$	$\hat{m}_3$	$\hat{n}_3$
±0.9919	±0.1270	0.0	∓0.1270	±0.9919	0.0
±0.9919	∓0.1270	0.0	∓0.1270	∓0.9919	0.0

then

$\hat{l}_\eta$	$\hat{m}_\eta$	$\hat{n}_\eta$	$\hat{l}_s$	$\hat{m}_s$	$\hat{n}_s$
±0.6116	±0.7912	0.0	±0.7912	∓0.6116	0.0
±0.6116	∓0.7912	0.0	±0.7912	±0.6116	0.0

The expected fatigue fracture plane positions are presented in Figs. 3Ia and 3IIa. In Figs.3Ib and 3IIb graphs of the function $\mu_{\sigma red}$ according to (12) are presented.

In the considered case we obtain two expected fatigue fracture planes for each material. They are parallel to the axis z and their positions vary depending on a material (influence of K).

4.3 Triaxial tension-compression

Suppose that all shear stresses vanish and only normal stresses are non-zero. This renders

$$\mu_{\sigma red}= \frac{1}{(1+K)^2} \{ [\hat{l}_1^2 - \hat{l}_3^2 + K(\hat{l}_1+\hat{l}_3)^2]^2 \mu_{x11} + [\hat{m}_1^2 - \hat{m}_3^2 + K(\hat{m}_1+\hat{m}_3)^2]^2 \mu_{x22} + [\hat{n}_1^2 - \hat{n}_3^2 + K(\hat{n}_1+\hat{n}_3)^2]^2 \mu_{x33} + 2[\hat{l}_1^2 - \hat{l}_3^2 + K(\hat{l}_1+\hat{l}_3)^2][\hat{m}_1^2 - \hat{m}_3^2 + K(\hat{m}_1+\hat{m}_3)^2] \mu_{x12} + 2[\hat{l}_1^2 - \hat{l}_3^2 + K(\hat{l}_1+\hat{l}_3)^2][\hat{n}_1^2 - \hat{n}_3^2 + K(\hat{n}_1+\hat{n}_3)^2] \mu_{x13} + 2[\hat{m}_1^2 - \hat{m}_3^2 + K(\hat{m}_1+\hat{m}_3)^2][\hat{n}_1^2 - \hat{n}_3^2 + K(\hat{n}_1+\hat{n}_3)^2] \mu_{x23} \} \qquad (13)$$

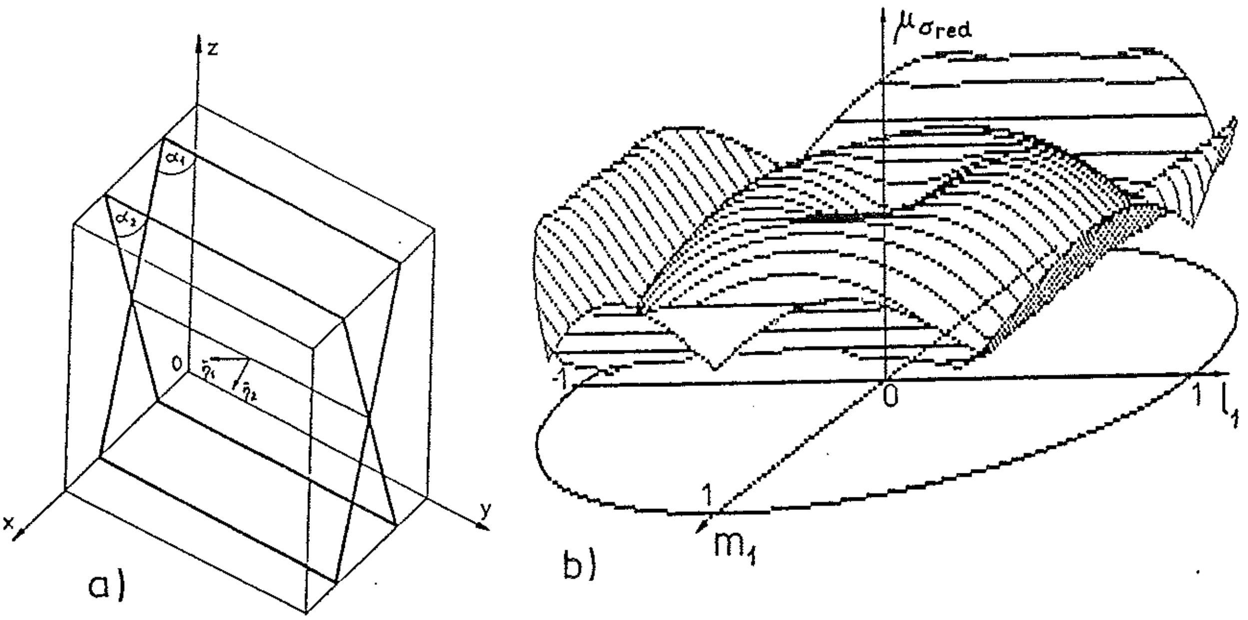

Fig. 4.I The expected fatigue fracture plane positions and a graph of variance function (according to (13)) for mild steel

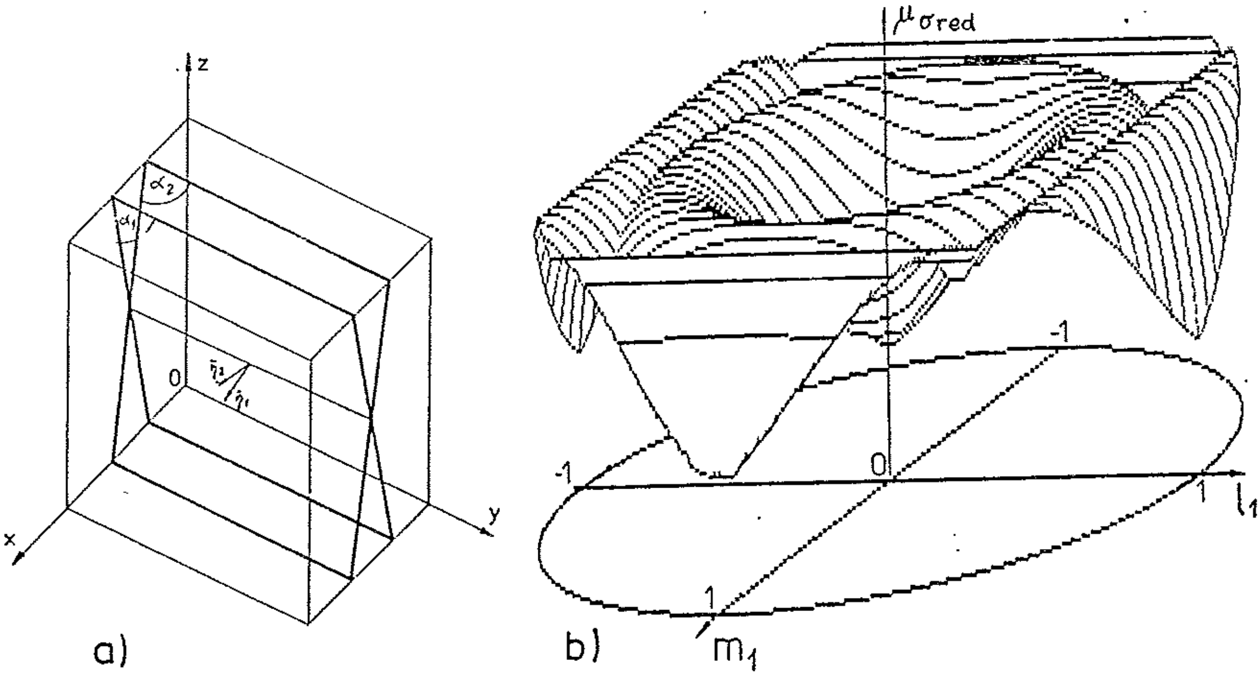

Fig.4.II. The expected fatigue fracture plane positions and a graph of variance function (according to (13)) for hard steel

The covariance matrix for this state of stress was

$$\underset{\approx}{\mu}_x = \begin{vmatrix} \mu_{x11} & \mu_{x12} & \mu_{x13} \\ \mu_{x21} & \mu_{x22} & \mu_{x23} \\ \mu_{x31} & \mu_{x32} & \mu_{x33} \end{vmatrix} = \begin{vmatrix} 3964 & 9 & -40 \\ 9 & 3877 & 90 \\ -40 & 90 & 3900 \end{vmatrix}$$

The obtained maximum of the function (13) was $\mu_{\sigma red}$=5631 MPa^2 for mild steel and 10352 MPa^2 for hard steel in the following points:

I.Mild steel

$\hat{l}_1$	$\hat{m}_1$	$\hat{n}_1$	$\hat{l}_3$	$\hat{m}_3$	$\hat{n}_3$
0.9409	0.0	∓0.3387	0.3387	0.0	±0.9409
-0.9409	0.0	±0.3387	-0.3387	0.0	∓0.9409

then

$\hat{l}_\eta$	$\hat{m}_\eta$	$\hat{n}_\eta$	$\hat{l}_s$	$\hat{m}_s$	$\hat{n}_s$
0.9048	0.0	±0.4258	0.4258	0.0	∓0.9048
-0.9048	0.0	∓0.4258	-0.4258	0.0	±0.9048

II. Hardened steel

$\hat{l}_1$	$\hat{m}_1$	$\hat{n}_1$	$\hat{l}_3$	$\hat{m}_3$	$\hat{n}_3$
0.7902	0.0	±0.6129	0.6129	0.0	∓0.7902
-0.7902	0.0	±0.6129	-0.6129	0.0	∓0.7902

$\hat{l}_\eta$	$\hat{m}_\eta$	$\hat{n}_\eta$	$\hat{l}_s$	$\hat{m}_s$	$\hat{n}_s$
0.9921	0.0	∓0.1253	0.1253	0.0	±0.9921
-0.9921	0.0	∓0.1253	-0.1253	0.0	±0.9921

The expected fatigue fracture plane positions determined by the method of variance are presented in Figs.4Ia and 4IIa. Figures 4Ib and 4IIb show graphs of the function $\mu_{\sigma red}$ according to (13).
Here two critical planes were obtained,as well. They are parallel to the axis y. However,there are many other sets of cosines $\hat{l}_i, \hat{m}_i, \hat{n}_i$ for which this function has a value slightly lower than the total maximum. Like in the previous cases,a distinct influence of a kind of material on the expected fatigue fracture plane position can be observed.

4.4 Triaxial tension-compression with triaxial shear

If all of six stress components are non-zero, then $\mu_{\sigma red}$ is given by equation (8).
The generated courses of stress state components give the following covariance matrix

$$\underset{\approx}{\mu}_x = \begin{vmatrix} 3913 & 22 & 47 & -43 & 25 & -16 \\ 22 & 3930 & 55 & -51 & -31 & 46 \\ 47 & 55 & 3960 & -10 & 65 & -27 \\ -43 & -51 & -10 & 3917 & 7 & 36 \\ 25 & -31 & 65 & 7 & 3899 & -8 \\ -16 & 46 & -27 & 36 & -8 & 3958 \end{vmatrix} \; MPa^2$$

From the optimization calculations for the function (8) the maximum value $\mu_{\sigma red}=10243\ MPa^2$ was obtained for mild steel and for hard steel $\mu_{\sigma red}=17541\ MPa^2$ was obtained in the following points

I. Mild steel

$\hat{l}_1$	$\hat{m}_1$	$\hat{n}_1$	$\hat{l}_3$	$\hat{m}_3$	$\hat{n}_3$
±0.3761	∓0.8488	±0.3712	±0.5620	±0.5271	±0.6373
±0.6342	∓0.3281	±0.7001	∓0.1805	∓0.9428	∓0.2802

then

$\hat{l}_\eta$	$\hat{m}_\eta$	$\hat{n}_\eta$	$\hat{l}_s$	$\hat{m}_s$	$\hat{n}_s$
±0.6633	∓0.2275	±0.7131	∓0.1315	∓0.9729	∓0.1882
±0.3208	∓0.8987	±0.2969	±0.5761	±0.4347	±0.6932

II. Hardened steel

$\hat{l}_1$	$\hat{m}_1$	$\hat{n}_1$	$\hat{l}_3$	$\hat{m}_3$	$\hat{n}_3$
±0.2481	∓0.9539	±0.1689	±0.6188	±0.2910	±0.7296
±0.7289	±0.0431	±0.6833	0.0	∓0.9981	±0.0616

$\hat{l}_\eta$	$\hat{m}_\eta$	$\hat{n}_\eta$	$\hat{l}_s$	$\hat{m}_s$	$\hat{n}_s$
±0.6130	∓0.4687	±0.6353	∓0.2621	∓0.8803	∓0.3965
±0.5154	∓0.6753	±0.5267	±0.5154	±0.7362	±0.4396

The expected fatigue fracture plane positions determined in such a way are presented in Figs.5Ia and 5IIa. In Figs.5Ib and 5IIb there are graphs of the function $\mu_{\sigma red}$ according to (8).

Two expected fatigue fracture plane positions were obtained for each considered material. They are probable to the same degree but, like in 4.3, from the graph of $\mu_{\sigma red}$ it appears that there are many other planes which are probable to a similar degree.

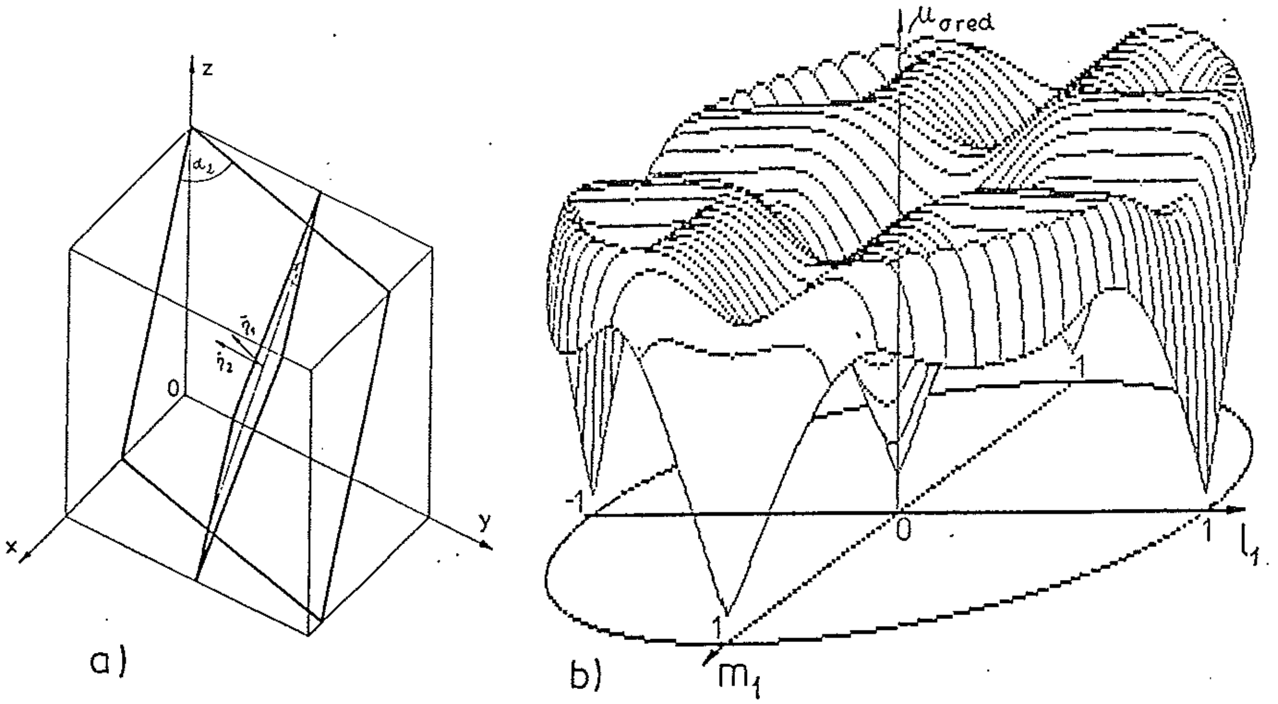

Fig.5I The expected fatigue fracture plane position and graph of variance function (according to (8)) for mild steel

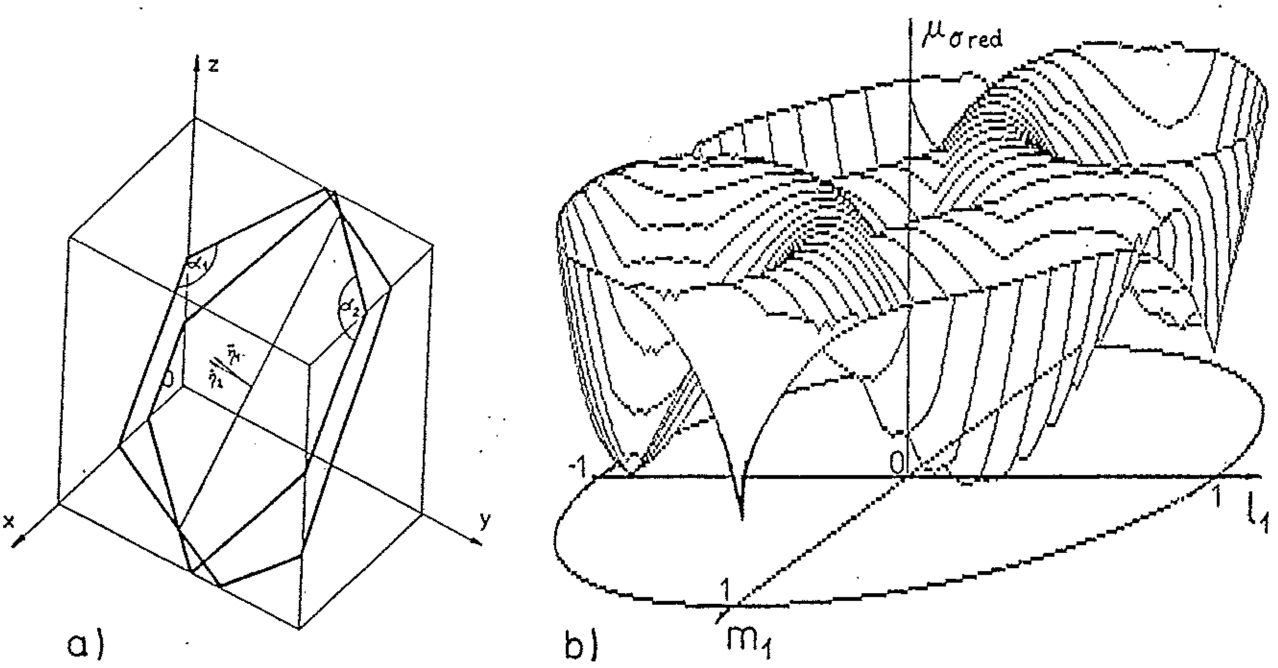

Fig.5II The expected fatigue fracture plane position and graph of variance function (according to (8)) for hard steeel

Generally speaking, for each considered case we can observe a distinct influence of coefficient K (a type of material) on the expected fatigue fracture plane position determined by the discussed method.

Equivalent maxima of the function $\mu_{\sigma red}$ appear in several directions, so each of these directions is probable in the same degree. Evaluation of fatigue life on the assumption that one of the distinguished planes is the expected fatigue fracture plane gives the same results.

5. VERIFICATION OF THE DISCUSSED METHOD BASING ON THE RESULTS OF CYCLIC FATIGUE TESTS

The analysis has been carried out on the basis of the results of tests discussed in [1,11,12]. Rotvel [12] tested cylindrical specimens under cyclic biaxial tension-compression with a phase shift. Nishihara & Kawamoto [11] examined round specimens made of four materials under torsion with bending at various ratios of amplitudes and phase shifts. Achtelik et al. [1] tested round specimens under synchronous bending and torsion. In the mentioned papers the fatigue fracture plane positions obtained for given loadings are presented. Owing to these data it was possible to compare the estimated fatigue fracture plane positions obtained with the method of variance and the experimental data. Absolute value of difference between their direction cosines, not higher than 0.1, was assumed as criterion of conformity. If two directions of fatigue fracture planes were obtained from theoretical considerations, the direction more similar to that obtained from experiments was assumed.

In the analysed cases of loading the following conformities with experimental data were obtained:

- for steel 0.35 % C [15] 100 %
- for hard steel (0.51 %) [3] 100 %
- for mild steel (0.1 %) [3] 100 %
- for duralumin (3.81 % Cu) [3] 50 %
- for cast iron (3.87 % C) [3] 33 %
- for cast iron ZL250 (3.32 % C) [3] 60 %

From these data it results that for carbon steel a very good conformity is obtained, irrespective of carbon content and a kind of heat treatment. A low conformity is obtained for duralumin and cast iron. A better conformity is obtained for these two materials if the mean direction of these two directions presented in tables is assumed as a theoretical direction of fatigue fracture plane. A full evaluation of correctness of the proposed method will be possible as a result of much more experiments, especially for multiaxial random loadings.

6. CONCLUSIONS

1. The variance method for determining the expected fatigue fracture plane position under multiaxial fatigue concerns states of stress, components of which are stationary and ergodic random processes.
2. In the variance method it is assumed that a plane in which variance of the equivalent stress reaches its maximum is critical for the material and fatigue fracture can be expected in this plane.
3. Application of the variance method for the criterion of maximum shear and normal stresses in case of four simulated multiaxial random states of stress gives two or more expected fatigue fracture planes and they are probable to the same degree.
4. From experimental data for multiaxial cyclic fatigue it appears that the variance method with the discussed stress criterion gives good results for three analysed types of carbon steels.
5. A full evaluation of the presented method will be possible after some new experiments for both cyclic and random multiaxial loadings.

REFERENCES

[1] Achtelik H., Macha E., Jakubowska I., Actual and estimated rections of fatigue fracture plane in ZL 250 grey cast iron under combined alternating bending and tension, Studia Geotechnica et Mechanica, Vol.V, No.2, 1983, pp.9-30.

[2] Będkowski W., Lachowicz C.T., Macha E., Predicted fatigue fracture plane according to variance of shear stress under triaxial stress state, ECF - 7, Budapest 1988, Proceedings of the 7th ECF, Vol.I, pp.281-283.

[3] Będkowski W., Macha E., Fatigue criterion of the maximum strain in direction perpendicular to a fracture plane, VDI Reiche 5, No.97, Dusseldorf 1985, p.94.

[4] Będkowski W., Macha E., Maximumm normal stress fatigue criterion applied to random triaxial stress state, Theoretical and Applied Fracture Mechanics, Vol.7, No.2,1987,pp.98 -107.

[5] Cox H.L., Field J.E., The initiation and propagation of fatigue cracks in mild steel pieces in square sections.The Aeronautical Quarterly, Vol.4, Aug.1952, pp.1-18.

[6] Findley W.N.,Coleman J.J.,Hanley B.C., Theory for combined bending and torsion fatigue with data for SAE 4340,Proc.Int. Conf.on Fatigue of Metals, London 1956, pp.150-157.

[7] Macha E,. Generalization of fatigue fracture criteria for multiaxial sinusoidal loadings in the range of random loadings, Biaxial and Multiaxial Fatigue EGF-3 (Edited by M.W. Brown and K.J.Miller), 1988, Mechanical Engineering Publications,London,pp.425-436.

[8] Macha E., Statistical characteristics of strains, principal stresses and direction cosines in random stress state,Studia Geotechnica et Mechanica,Vol.VII, No.2, 1984, pp.21-54.

[9] Macha E., The expected positions of fatigue fracture planes according to analytical methods, Inter.Conf.on Fracture ECF-6, Amsterdam 1986, poster session.

[10] Miller K.J., Brown M.W., Multiaxial fatigue -an introductory review, Courses on Mechanical Science and Materials, Ed.L.H. Larson, Joint Research Centre,Ispra, Italy,1981,pp.215-238.

[11] Nishihara T.,Kawamoto M.,The strength of metals under combined alternating bending and torsion with phase difference, Memoirs of the College of Engineering, Kyoto Imperial University, Vol.XI, No.4, 1945, pp.95-112.

[12] Rotvel F.,Biaxial fatigue tests with zero mean stresses using tubular specimens,Int.J.of Mech.Sc.,Pergamon Press,Vol. 12, 1970, pp.597-615.

[13] Socie D.F.,Multiaxial fatigue damage assesment,low-cycle fatigue and elastoplastic behaviour of materials, Ed.K.T.Pie, Elsevier Applied Science, London 1987, pp.465-472.

[14] Stulen F.B.,Cummings H.N., A failure criterion for multiaxial fatigue stresses, Proc.ASTM, Vol.54, Philadelphia 1954, pp.822-835.

[15] Zamrik S.Y., Frismuth R.E., The effect of out of phase biaxial strain cyclic on low-cycle fatigue, Experimental Mech. May 1973, pp.204-208.